PROCEEDINGS OF SCIENCE

Performance of missing transverse momentum reconstruction at the CMS detector in 13 TeV data

Leonora Vesterbacka Olsson[*†]
ETH Zürich
E-mail: leonora.vesterbacka@cern.ch

The precise measurement of the missing transverse momentum (p_T^{miss}) observable is critical for standard model measurements involving W, Z, and the Higgs bosons, and top quarks. In addition, p_T^{miss} is one of the most important kinematic observables used in searches for physics beyond the standard model targeting new weakly interacting neutral particles. A detailed understanding of various effects due to the high collision rate at the CMS detector during the 13 TeV data-taking period of the LHC both in data and simulation is important to achieve the most optimal p_T^{miss} performance. In this talk, we will present studies of p_T^{miss} reconstruction algorithms using the CMS detector at the LHC.

ICHEP 2018, International conference on High Energy Physics
4-11 July 2018
Seoul, South Korea

[*]Speaker.
[†]on behalf of the CMS Collaboration

PoS(ICHEP2018)250

1. Introduction

Neutrinos and hypothetical neutral weakly interacting particles can be produced in proton-proton (pp) collisions at the Large Hadron Collider (LHC) at CERN. As these particles rarely interact with usual matter, they leave no signal in the detector, and their existence can only be inferred through the momentum imbalance in the plane perpendicular to the beam direction. The CMS detector at the LHC has the possibility to precisely measure physics objects such as e, μ, τ, γ, jets, and these reconstructed objects are used in the determination of the missing transverse momentum ($\mathrm{p_T^{miss}}$). In CMS, two $\mathrm{p_T^{miss}}$ reconstruction algorithms are most commonly used, the Particle Flow (PF) and 'pileup per particle identification' (PUPPI) [1] $\mathrm{p_T^{miss}}$. The performance of these two algorithms is crucial for any SM or Higgs measurement, or any search for physics beyond the SM. This document presents the performance studies using $35.9\,\mathrm{fb}^{-1}$ pp collision data collected by the CMS experiment in 2016 at a center-of-mass energy of 13 TeV.

2. $\mathrm{p_T^{miss}}$ reconstruction

The first $\mathrm{p_T^{miss}}$ reconstruction algorithm based on the PF event description is referred to as PF $\mathrm{p_T^{miss}}$, and is defined as the negative vector sum of the $\mathrm{p_T}$ of all the PF candidates in an event. This algorithm is used in the majority of the CMS analysis and provides a robust $\mathrm{p_T^{miss}}$ reconstruction. The second method relies on the PUPPI algorithm which is a technique that aims to reduce the pileup dependence of jets and $\mathrm{p_T^{miss}}$ by re-weighting each PF candidate in an event according to how likely the candidate is to be originating from pileup. The PUPPI $\mathrm{p_T^{miss}}$ is determined as the magnitude of the negative vectorial sum of the re-weighted PF candidates. The energy scale of the both $\mathrm{p_T^{miss}}$ algorithms are improved by propagating the Jet Energy Corrections (JECs), used to correct the $\mathrm{p_T}$ of the jets to the true particle level jets, to the $\mathrm{p_T^{miss}}$ itself. The corrected $\mathrm{p_T^{miss}}$ used throughout this document, and is referred to as the Type-1 $\mathrm{p_T^{miss}}$ in some of the subsequent figures. The uncertainties related to the measurement of the $\mathrm{p_T^{miss}}$ are dominated by the measurement of the jets. By recalculating the $\mathrm{p_T^{miss}}$ after varying the jet energy scale (JES), jet energy resolution (JER) and unclustered energy (UE) by their uncertainties, the magnitude of the uncertainty on the $\mathrm{p_T^{miss}}$ can be estimated as the difference between the recalculated $\mathrm{p_T^{miss}}$ and the nominal $\mathrm{p_T^{miss}}$. In the following studies, the systematic uncertainty due to the JES, the JER, and variations in the UE are added in quadrature and displayed with a band in the data to simulation ratio.

3. $\mathrm{p_T^{miss}}$ performance

The performance of the $\mathrm{p_T^{miss}}$ algorithm can be assessed in events where no genuine $\mathrm{p_T^{miss}}$ is present, i.e. in events where no neutrinos are produced and the $\mathrm{p_T^{miss}}$ is originating solely from jet mismeasurements or detector inefficiencies. For this, di-muon, di-electron and single photon events are used, in which the majority of events have a single Z boson decaying leptonically, or γ produced with jets recoiling off of the boson. The performance of the $\mathrm{p_T^{miss}}$ algorithms can be assessed by studying the so-called $\mathrm{p_T^{miss}}$ response and resolution. Events with no genuine $\mathrm{p_T^{miss}}$ are selected, and the hadronic recoil, u, is projected on to the axis of the well measured boson. The parallel and perpendicular components of the $\mathrm{u_T}$ are denoted $\mathrm{u_{||}}$ and $\mathrm{u_\perp}$ respectively. The $\mathrm{p_T^{miss}}$

response is defined as $-\langle u_{||}\rangle/\langle q_T\rangle$ and the resolution is the RMS of the $u_{||}$ and $u_\perp$, measured as a function of boson p_T (denoted q_T in the following) and number of vertices.

3.1 PF p_T^{miss} performance

The PF p_T^{miss} in events with no genuine p_T^{miss} are shown in Fig. 1 and show a good agreement between the data and the simulated events. The p_T^{miss} response and resolution as a function of q_T

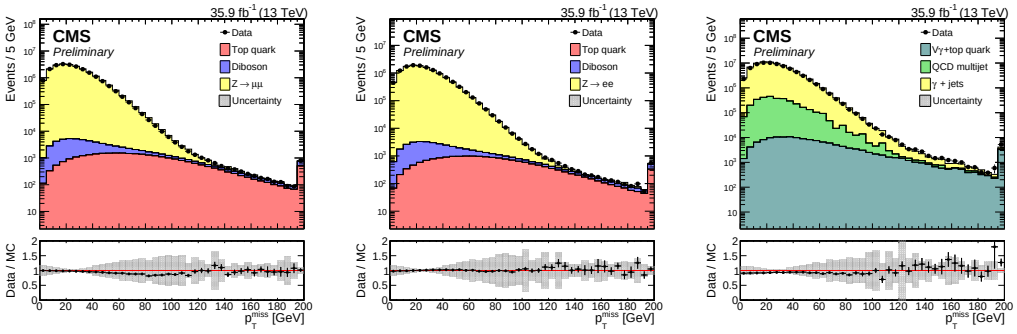

Figure 1: PF p_T^{miss} in $Z \to \mu\mu$ (left), $Z \to ee$ (middle), and γ+jets events (right) in data and simulation [2].

are shown in Fig. 2. The response show a good agreement between the three event selections, the data and the simulation, and is reaching unity at q_T of around 100 GeV. The resolution of the $u_{||}$ displays and increase with higher q_T, whereas a flat behaviour is observed for the resolution of the $u_\perp$ as this component is more sensitive to isotropic effects rather than the scale of the boson.

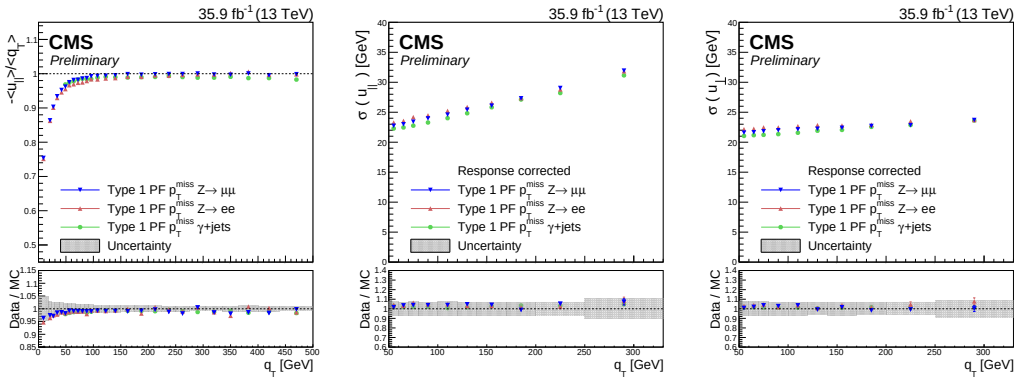

Figure 2: The p_T^{miss} response (left), the resolution $u_{||}$ (middle) and $u_\perp$ as a function of q_T, in $Z \to \mu\mu$, $Z \to ee$, and γ+jets events [2].

3.2 PUPPI p_T^{miss} performance

The PUPPI p_T^{miss} in events with no genuine p_T^{miss} are shown in Fig. 3 and show a good agreement between the data and the simulated events. The PUPPI p_T^{miss} response is shown in Fig. 4. The response show a good agreement between the two event selections, the data and the simulation, and is reaching unity at q_T of around 150 GeV. As the PUPPI p_T^{miss} algorithm is developed to ensure a high performance in higher pileup scenarios, the resolution obtained using the PF and PUPPI p_T^{miss}

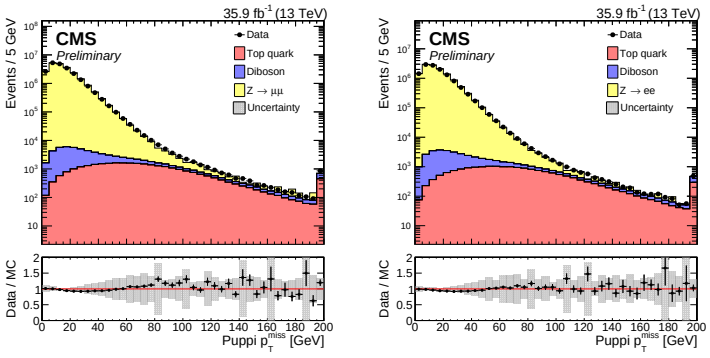

Figure 3: The PUPPI p_T^{miss} in $Z \to \mu\mu$ (left), $Z \to ee$ (right), in data and simulation [2].

algorithms as a function of number of vertices are compared in Fig. 4. The resolution of the PF p_T^{miss} algorithm is increasing with higher number of vertices, whereas a flat behaviour is observed for the PUPPI p_T^{miss}.

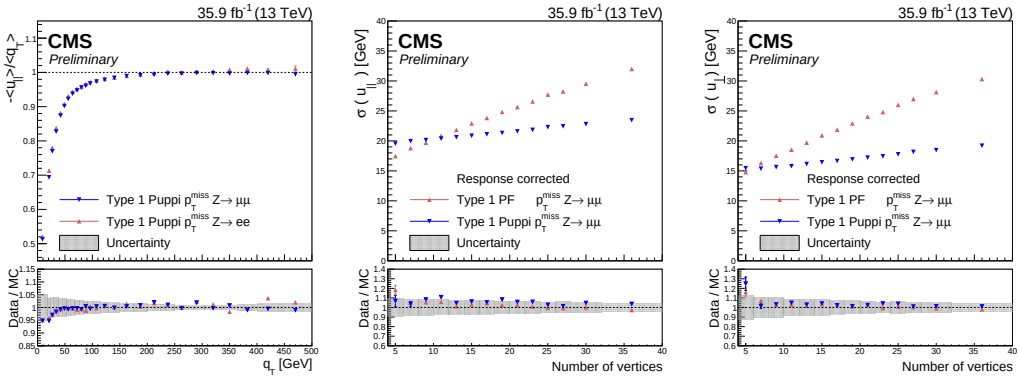

Figure 4: The p_T^{miss} response (left), the resolution $u_{||}$ (middle) and $u_\perp$ as a function of q_T, in $Z \to \mu\mu$, $Z \to ee$, and γ+jets events [2] .

4. Summary

This document presents the performance of the PF and PUPPI p_T^{miss} algorithms using pp data collected in 2016 corresponding to an integrated luminosity of 35.9 fb^{-1} at a center-of-mass energy of 13 TeV. The two algorithms are evaluated in events with no genuine p_T^{miss}, and show a good agreement between the data and the simulation, and between the different event selections. Additionally, the PUPPI p_T^{miss} has factor of 2 less resolution degradation at each additional vertex compared to PF p_T^{miss} .

References

[1] D. Bertolini, P. Harris, M. Low and N. Tran, "Pileup Per Particle Identification," JHEP **1410**, 059 (2014) doi:10.1007/JHEP10(2014)059 [arXiv:1407.6013 [hep-ph]].

[2] CMS Collaboration, "Performance of missing transverse momentum in pp collisions at $\sqrt{s} = 13$TeV using the CMS detector," CMS-PAS-JME-17-001 [http://cds.cern.ch/record/2628600]